XVI International Conference on Durability of Building Materials and Components
DBMC 2023, China
K.F. Li and D.P. Fang (Eds)

Accelerating Effect of Heating Treatment on the Damage of Cement Paste under Sulfate Attack

Bo Ran[1,2], Othman Omikrine Metalssi[2], Teddy Fen-Chong[2], Patrick Dangla[3] and Kefei Li[1]

[1]Department of Civil Engineering, Tsinghua University, Beijing 100084, PR China, rb17@mails.tsinghua.edu.cn (Bo Ran), likefei@tsinghua.edu.cn (Kefei Li)

[2]Cerema, UMR MCD, Univ. Gustave Eiffel, Marne-la-Vallée, F-77454, France, teddy.fen-chong@uni-eiffel.fr (Teddy Fen-Chong), othman.omikrine-metalssi@univ-eiffel.fr (Othman Omikrine-Metalssi)

[3]Navier, Ecole des Ponts, Univ. Gustave Eiffel, CNRS, Marne-la-Vallée, F-77447, France, patrick.dangla@univ-eiffel.fr (Patrick Dangla)

Abstract. *The ettringite (AFt) formation and damage process are investigated for cement paste subjected to external sulfate attack with and without heating treatment during curing. Slice and disc specimens were exposed to 10 g/L Na_2SO_4 + pH of 13. The evolutions of AFt formation, pore structure, and expansion on slice specimens were characterized through ^{27}Al NMR, MIP, and micrometer. The surface cracks on disc specimens were observed through an optical microscope. The experimental results show that: (1) heating treatment dissolves part of AFt and accelerates the ettringite formation and material expansion; and (2) heating treatment initiates the microcracks, thus promoting the material cracking.*

Keywords: *Cement Paste, Sulfate Attack, Heating Treatment, Ettringite, Damage.*

1 Introduction

For massive concrete, the interior is usually cured at high temperature, which may exceed 70°C (Divet and Randriambololona, 1998) due to the slow dissipation of the hydration heat. The elevated temperature causes the decomposition of the formed ettringite and the release of sulfates and aluminium into pore solution in the early curing period. Afterwards, the released ions recrystallize in the hardened concrete matrix during the later cooling stage, and the recrystallization in the matrix generates crystallization pressure and may lead to concrete deterioration, which is known as delayed ettringite formation (DEF) (Taylor et al., 2001).

The mechanism of DEF has been well investigated in the literature. According to Yang et al. (1999), the expansion of specimens subjected to DEF occurs as an S-shape curve, and the expansion value ceases to increase once the released sulfate is consumed. Several models have been proposed to simulate the DEF damage: Flatt and Scherer (2008) proposed a thermodynamic model to estimate the hydrostatic tensile stress in the pore solution; Brunetaud (2005) suggested a parametric model to estimate the expansion induced by DEF, and Gu et al. (2022) developed a poromechanical model based on an interface-controlled crystal growth mechanism to simulate the ettringite formation and expansion growth.

Besides the DEF, there is a possibility of having both external sulfate attack (ESA) and DEF in some circumstances. For example, a massive concrete component is completely buried in an

environment containing sulfates, such as saline soil or some groundwater. In this case, the sulfates for AFt formation after the hardening of cement paste originate from both the external environment and the released sulfates as an internal source. Therefore, the combined condition is the most detrimental and should be considered for the massive concrete exposed to ESA. In the literature, however, few studies have been conducted on this topic. To this objective, this study designs two kinds of cement pastes (one with and one without heating treatment), and characterizes their damage processes under sulfate solution.

2 Experimental Program

2.1 Specimen Preparation

A CEM I Type (CEMI 52.5 N CE CP2) is used in this study to prepare cement paste with a water-to-cement ratio of 0.55, and the chemical composition of the cement is given in Table 1. Prisms of 40mm×40mm×160mm and cylinders of Φ110mm×220mm were farbricated from cement paste. Half of the paste underwent a 7-day heating procedure as described in Ref. (Martin, 2010) to simulate the temperature history of massive concrete in engineering, and the residual pastes were retained as the reference specimen. The reference pastes, named "ESA", together with the heating treated pastes (named "ESA + HT") were cured in a saturated CH solution to avoid leaching for 60 days. Rectangular slices of 2mm×20mm×120mm and square slices of 2mm×40mm ×40mm were cut from prisms, and disks of Φ110mm ×50mm were cut from cylinders. For the rectangular slices, a pair of pins were fixed on the two ends for expansion measurement. For the disks, an epoxy resin was glued on the lateral and bottom surfaces to leave the top surface subjected to sulfate penetration. All the prepared specimens were immersed in a sulfate solution of 10g/L SO_4^{2-} in Na_2SO_4. The test solution was kept at a pH of 13 by adding 0.1 M NaOH to avoid the leaching process during sulfate attack and was renewed weekly for the first month and biweekly thereafter. At given immersion ages, the square slices were subjected a freeze-drying treatment before the ^{27}Al NMR, XRD, and MIP tests; the rectangular slices were taken out for expansion measurement and then re-immersed into test solution, and the disks were cut diametrically to obtain two cross-sections for the cracking observation by optical microscope.

Table 1. Chemical composition of OPC.

					Components %			
CaO	SiO	Al_2O_3	Fe_2O_3	CaO(free)	MgO	SO_3	K_2O	Na_2O
62.8`	20.22	4.85	2.92	1.58	0.84	2.88	0.77	0.34

2.2 Experimental Methods

The experiments in this study include the 27Al NMR and XRD for the identification of mineral phases, MIP for microstructure characterization, micrometer for expansion measurement, and optical microscope for cracking observation.

2.2.1 ^{27}Al NMR

The device for the 27Al NMR test was a JNM-ECR600R Solid NMR Spectrometer with a field

intensity of 14.09 T. A tube of 3.2mm in diameter with a high spinning frequency of 15 kHz was adopted.

2.2.2 X-ray diffraction

The device for XRD analysis was a D/max-2550 (Bruker), and the XRD tests were performed on powder samples passing through a sieve of 80μm, using Cu radiation at an angular step of 0.02o per second between 5o and 75o [2θ].

2.2.3 Mercury intrusion porosimetry

The device for the MIP test was a Micromeritics' AutoPore (IV 9500 series) and the intrusion pressure was set in the range between 3.5kPa-414 MPa, corresponding to intruded pore diameters of between 400μm-3.7nm in hardened cement pastes.

2.2.4 Micrometer

The expansion was measured on the rectangular slice specimens, and the initial distance between the two pins on the rectangular slices was set at 100mm. The micrometer used for expansion measurement was detailed in Gu's work (Gu et al., 2019).Each measurement was performed three times, and a mean value was used.

2.2.5 Optical microscope

The device for the cracking observation test was an Olympus GX51 Inverted Metallurgical Microscope with a magnification of 10x of the objective lens in this study, and the observation was conducted along the penetration direction of sulfates into paste specimens.

3 Results and Analysis

3.1 Aluminium Phases

Following the multi-peaks fitting approach in the previous publications (De Lacaillerie et al., 2008; Ran et al., 2023), the NMR spectra were decomposed to obtain the relative ettringite content, and the results are presented in Figure 1. Figure 1 clearly demonstrates the accelerating effect of heating treatment on ettringite formation during external sulfate attack. Besides, the lower AFt content of the ESA+HT specimen at 0-day indicates the dissolution of AFt by the heating treatment. Figure 2 shows the XRD analysis of the 0-day speciemens and the results confirm the dissolution of AFt in the ESA+HT specimen. The more rapid AFt formation rate in ESA+HT specimens can be attributed to two effects of the heating treatment: the dissolved AFt releases sulfates into the pore solution, thereby increasing the ettringite supersaturation and formation rate; the released aluminium and sulfates after heating treatment are more uniformly distributed, resulting in a faster micro-diffusion of reaction ions to crystallization sites.

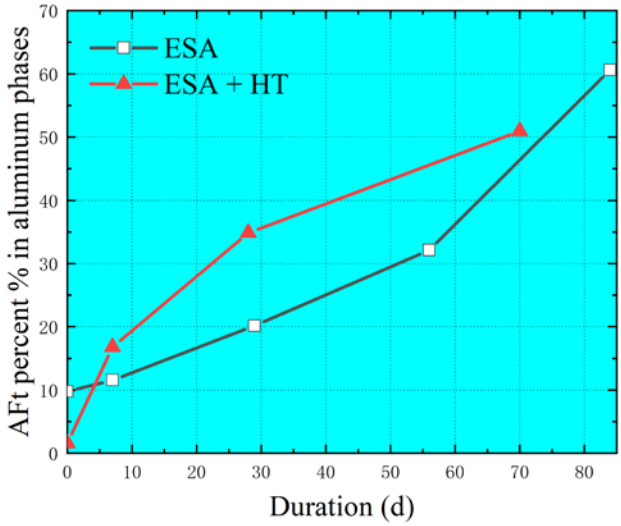

Figure 1. Comparison of AFt content with exposure time for slice specimens of ESA and ESA + HT.

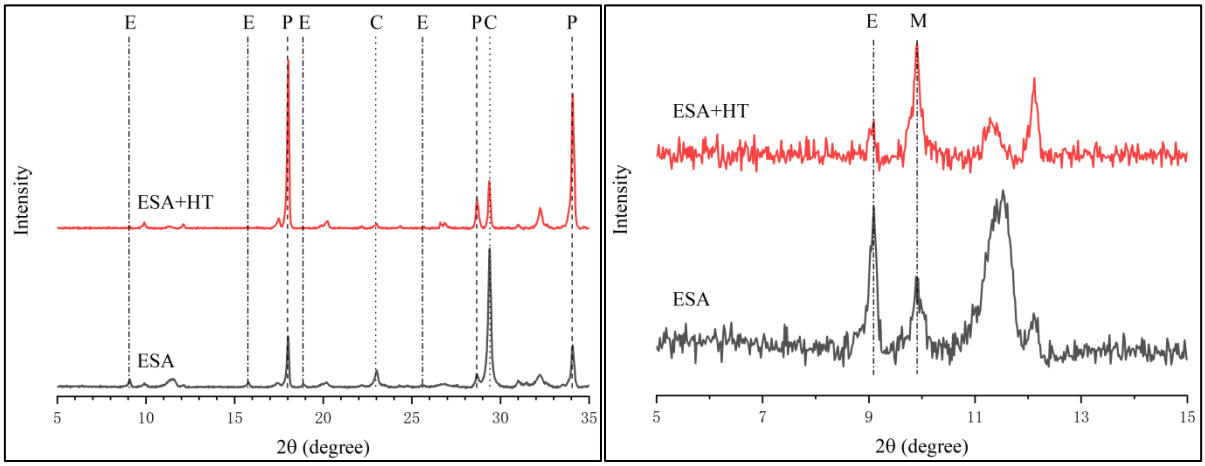

(a) (b)

Figure 2. XRD analysis of ESA and ESA+HT slice specimens before immersion (a) and zoom (b). “E”, “P”, “C” and “M” stand for ettringite, portlandite, calcite and monosulfoaluminate.

3.2 Pore Structure

Figure 3 presents the MIP results of ESA and ESA+HT specimens exposed to sulfate solution at different immersion ages. From Figure 3a, the interhydrate pore (around 20nm) volume decreases and the capillary pore (around 100nm) volume increases with time for ESA specimens. For the ESA+HT specimens in Figure 3b, the interhydrate and capillary pore volumes change similarly to those for the ESA specimens. Besides, a peak around 400-1000 nm appears in ESA+HT specimens and grows with time, indicating more severe damage on the pore structure of specimens after heating treatment. Figure 3c compares the pore size distribution (PSD) of ESA and ESA+HT specimens before immersion. After heating treatment, the two narrow peaks around 20nm and 100nm transform into a broad peak in the range between 10-1000 nm, with a significant increase in the pore space about 200-1000 nm, which suggests

the initiation of microcracks by the heating treatment during curing.

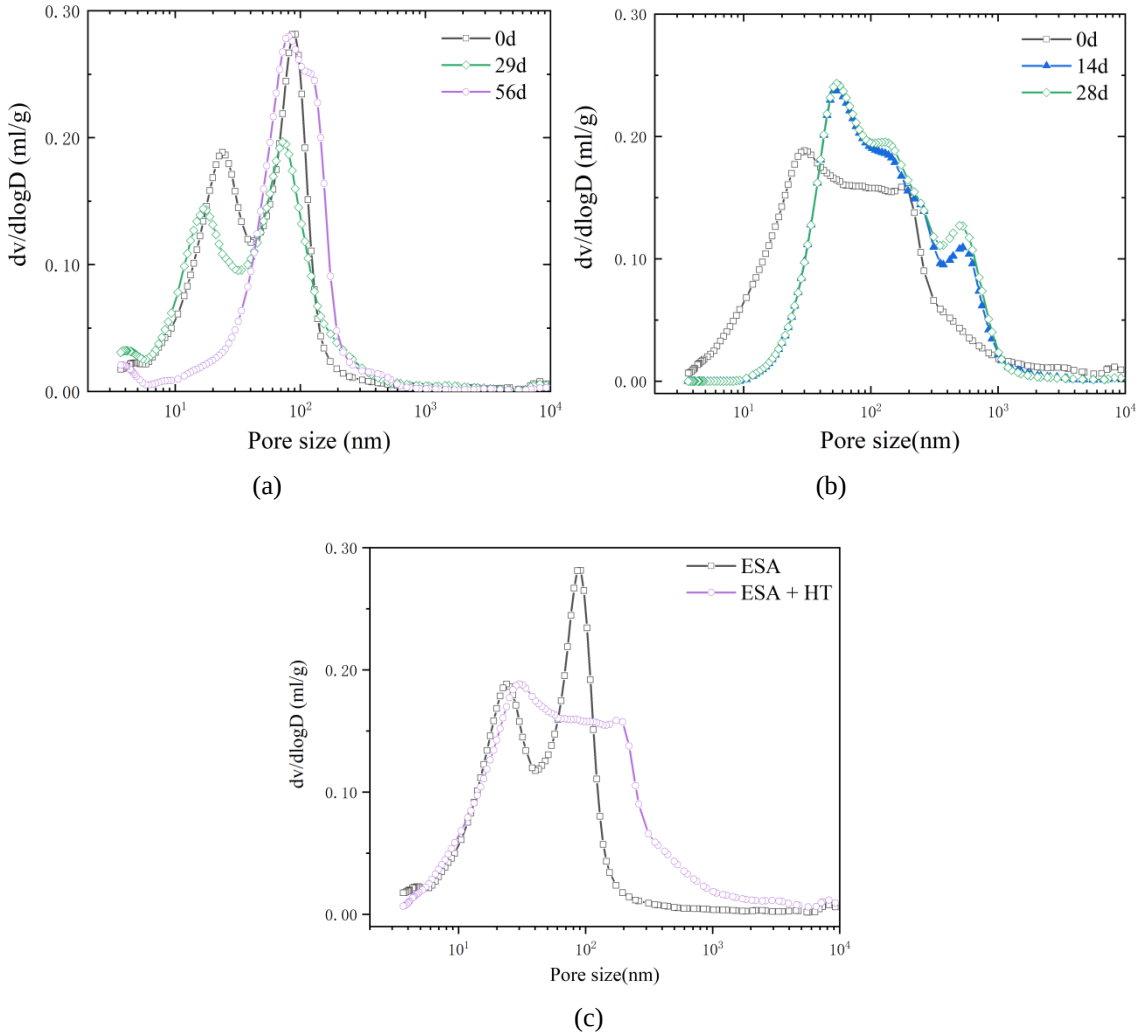

Figure 3. Evolution of pore size distribution (PSD) of ESA (a) and ESA+HT (b) slice specimens immersed into sulfate solution, and comparison of the PSD between ESA and ESA+HT at 0-day (c).

3.3 Expansion and Surface Cracking

Figure 4 shows the expansion results of ESA and ESA+HT specimens. Both expansion curves of ESA and ESA+HT specimens occur in two stages: an induction stage with a relative slow growth rate of expansion and a damage stage with a fast expansion rate. The expansion of slice specimens with heating treatment entered the damage stage earlier. Figure 5 presents the cracks on the cross-sections of ESA and ESA+HT disk specimens exposed to sulfate solutions at different immersion ages. There are no obvious cracks until 4-month immersion in ESA specimens, while ESA+HT specimens show visible cracks perpendicular to the exposure surface, which suggests much more severe damage in paste specimens with heating treatment subjected to sulfate penetration and agrees with the MIP results in Figure 3b.

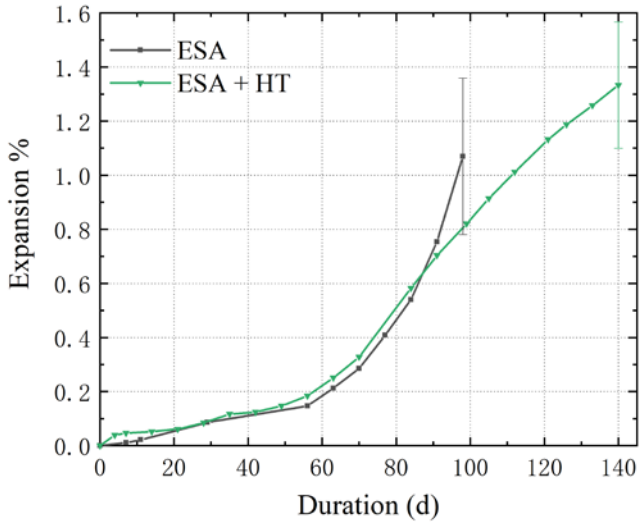

Figure 4. Expansion of ESA and ESA+HT slice specimens immersed into sulfate solution.

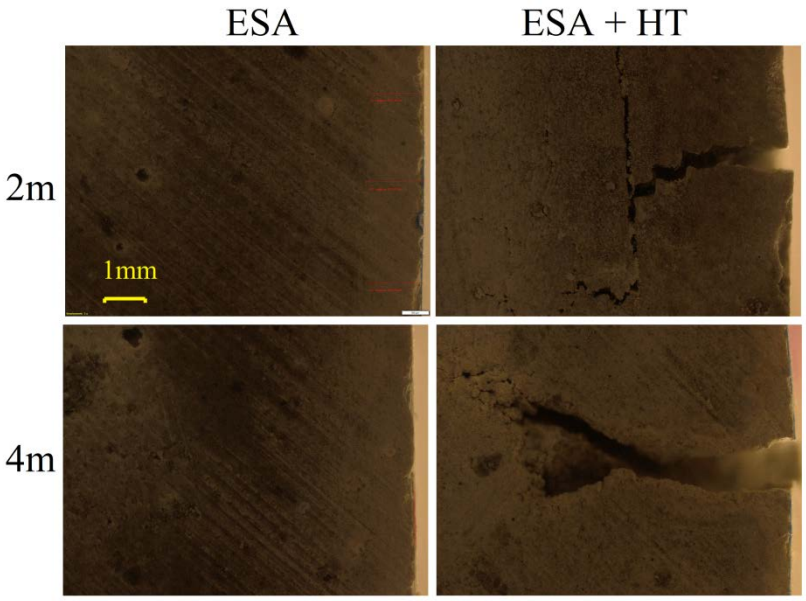

Figure 5. Cracking observation cross-sections of ESA and ESA+HT disk specimens exposed to sulfate solution.

4 Conclusions

- Heating treatment dissolves the initial AFt phase formed in the early curing period during the later cooling period and accelerates the AFt formation of paste specimens under external sulfate attack due to the release of sulfates and aluminium into the pore solution.
- Heating treatment initiates the microcracks of paste specimens, and promotes the development of microcracking behavior in MIP curves. Accordingly, heating treatment leads to faster expansion and more severe crack damage.

Acknowledgements

The research is supported by China National Science Foundation Grant No. 52038004.

References

Brunetaud, X. (2005). *Étude de l'influence de différents paramètres et de leurs interactions sur la cinétique de l'amplitude de la réaction sulfatique interne au béton* (Doctoral dissertation, Châtenay-Malabry, Ecole centrale de Paris).

De Lacaillerie, J. B. D. E., Fretigny, C., & Massiot, D. (2008). *MAS NMR spectra of quadrupolar nuclei in disordered solids: The Czjzek model*. Journal of Magnetic Resonance, *192*(2), 244-251.

Divet, L., & Randriambololona, R. (1998). *Delayed ettringite formation: the effect of temperature and basicity on the interaction of sulphate and CSH phase*. Cement and Concrete Research, 28(3), 357-363.

Flatt, R. J., & Scherer, G. W. (2008). *Thermodynamics of crystallization stresses in DEF*. Cement and Concrete Research, 38(3), 325-336.

Gu, Y., Dangla, P., Martin, R. P., Metalssi, O. O., & Fen-Chong, T. (2022). *Modeling the sulfate attack induced expansion of cementitious materials based on interface-controlled crystal growth mechanisms*. Cement and Concrete Research, 152, 106676.

Gu, Y., Martin, R. P., Metalssi, O. O., Fen-Chong, T., & Dangla, P. (2019). *Pore size analyses of cement paste exposed to external sulfate attack and delayed ettringite formation*. Cement and Concrete Research, 123, 105766.

Martin, R. P. (2010). *Analyse sur structures modèles des effets mécaniques de la réaction sulfatique interne du béton* (Doctoral dissertation, Université Paris-Est).

Ran, B., Omikrine-Metalssi, O., Fen-Chong, T., Dangla, P., & Li, K. (2023). *Pore crystallization and expansion of cement pastes in sulfate solutions with and without chlorides*. Cement and Concrete Research, 166, 107099.

Taylor, H. F. W., Famy, C., & Scrivener, K. L. (2001). *Delayed ettringite formation*. Cement and concrete research, 31(5), 683-693.